An Adaptive Learning-by-Examples Methodology for Accurate Crack Characterization in NDT-NDE Problems

M. Salucci, N. Anselmi, G. Oliveri, and A. Massa

Abstract

This document presents an adaptive learning-by-examples (*LBE*) inversion strategy for the accurate and real-time characterization of a defect within a planar conductive structure. More precisely, the developed technique exploits a Partial Least Squares (*PLS*) linear feature extraction strategy in order to *compress* the relevant information about the underlying relationship between defect and measurements into a small set of predictive features. Successively, an innovative adaptive sampling strategy is exploited in order to collect a set of *N* input-output (*I/O*) training pairs such that an *even exploration* of the *PLS*-extracted feature space is obtained. Such a training database is then used to train a Support Vector Regressor (*SVR*) for building an accurate and robust estimator of the crack dimensions starting from *ECT* measurements. Some numerical results are shown in order to validate the proposed approach also when a non-negligible amount of noise is superimposed on testing data.

1 Crack Dimensions Estimation Inside a Plate Structure

1.1 $PLS - OSF - SVR$ (Algorithm #3): Analysis for $J = 5$ - Performances

1.1.1 Parameters

- **Measurement set-up for the inversion**
  - considered measurement step: $\Delta_x = \Delta_y = 0.5$ [mm];
  - number of considered measurement points $K = K_x \times K_y = 5 \times 31 = 155$;
  - measured quantity for each k-th point: $\{\Re(\Psi_k), \Im(\Psi_k)\}$;
  - total number of measured features: $F = 2 \times K = 310$;

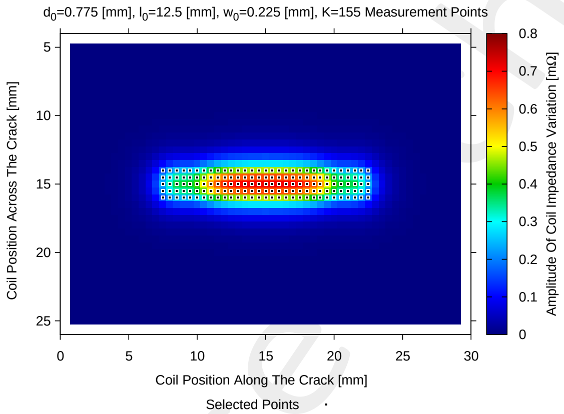

Figure 1: Location of the measurement points selected for the inversion ($K = 155$).

- $PLS - OSF - SVR$ **(algorithm #3)**
  - Initial training set (uniform grid)
    - Number of quantization levels: $Q_{x_0} = Q_{y_0} = Q_{z_0} = 5$;
    - Number of initial training samples: $N_1 = Q_{d_0} \times Q_{l_0} \times Q_{w_0} = 125$;
  - Number of extracted PLS components: $J = 5$;
  - SNR on training measurements: noiseless data;
  - Number of candidate samples: $C = 150$ $(50 \times I)$ (generated via LHS sampling);
  - SNR on training data: Noiseless;
  - Test set generation
    - Sampling: Latin Hypercube Sampling (LHS);
    - Number of test samples: $M = 1000$;
    - SNR on test data: Noiseless + $SNR = \{40; 30; 20; 10\}$ [dB].

1.1.2 Estimation of d_0

$SNR = 30$ [dB] on ECT Measurements

$N = 125$

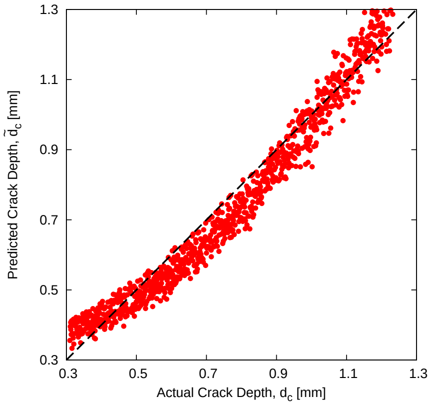

(a)

$N = 512$

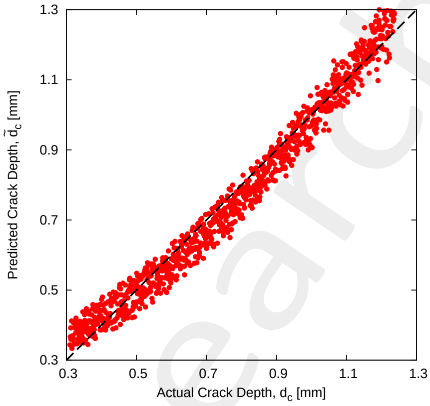

(b)

$N = 1000$

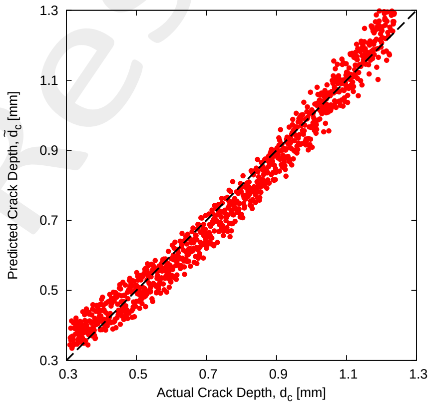

(c)

Figure 2: **PLS-OSF-SVR** - Actual vs. predicted depth of the crack for different values of N. $SNR = 30$ [dB] on test ECT data.

1.1.3 Estimation of l_0

$SNR = 30$ [dB] on ECT Measurements

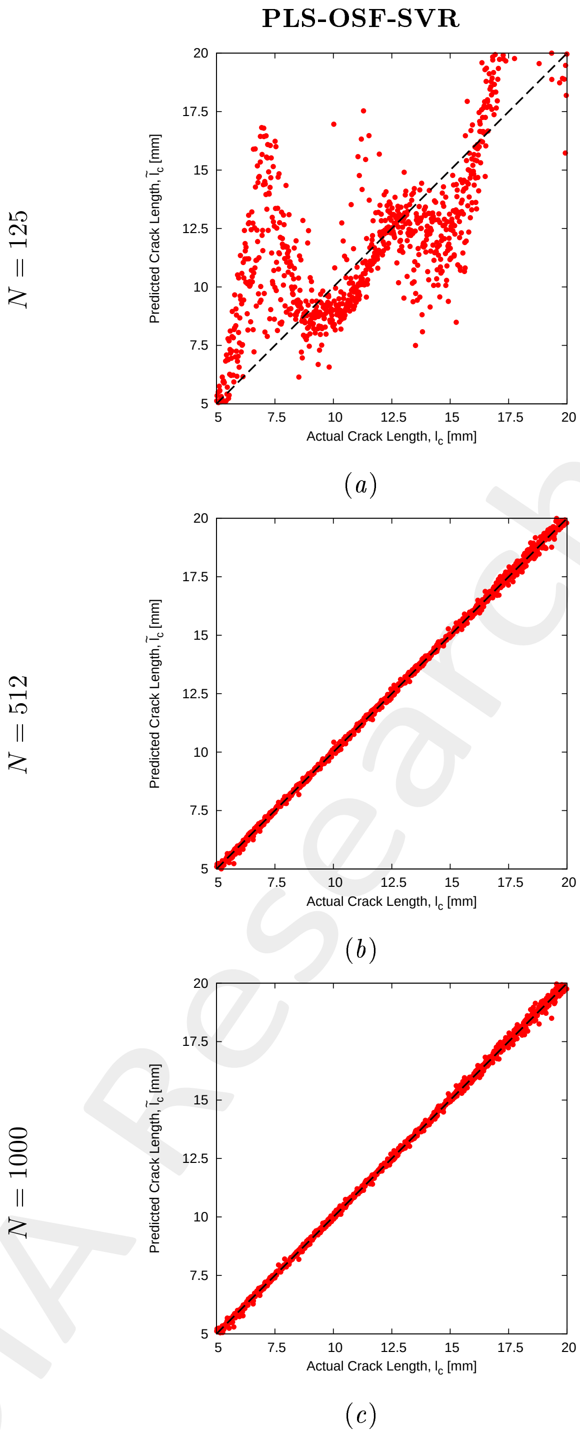

Figure 3: **PLS-OSF-SVR** - Actual vs. predicted length of the crack for different values of N. $SNR = 30$ [dB] test ECT data.

1.1.4 Estimation of w_0

$SNR = 30$ [dB] on ECT Measurements

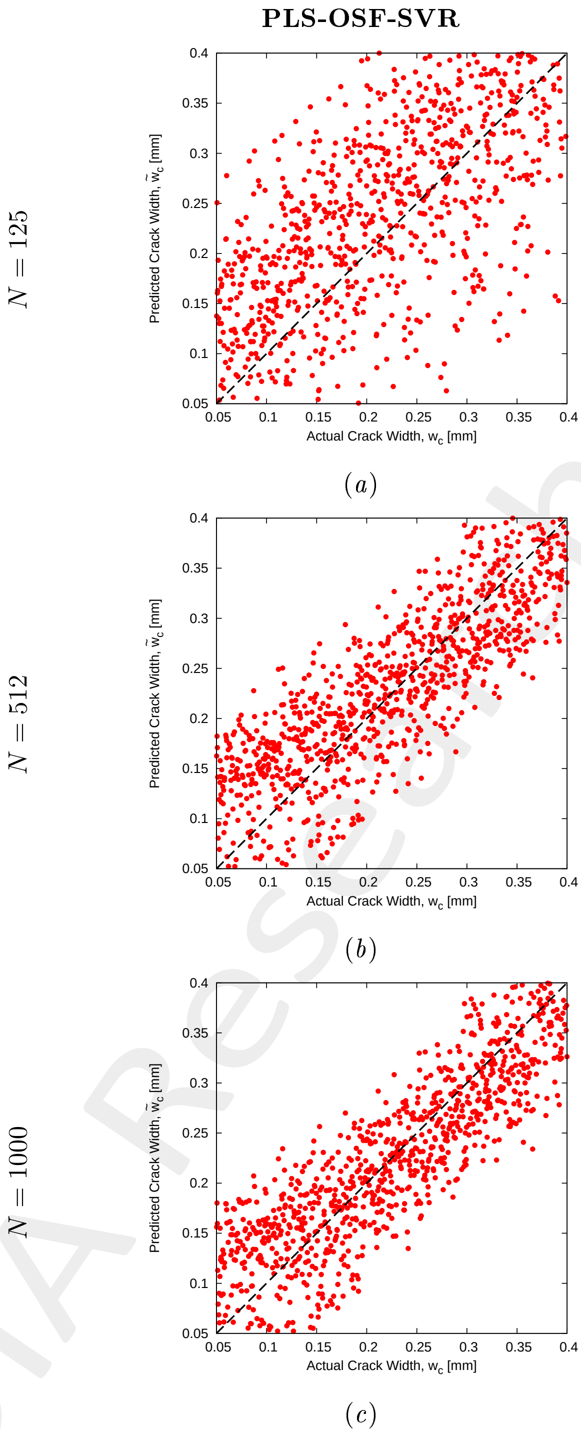

Figure 4: **PLS-OSF-SVR** - Actual vs. predicted width of the crack for different values of N. $SNR = 30$ [dB] on test ECT data.

1.1.5 Prediction Errors

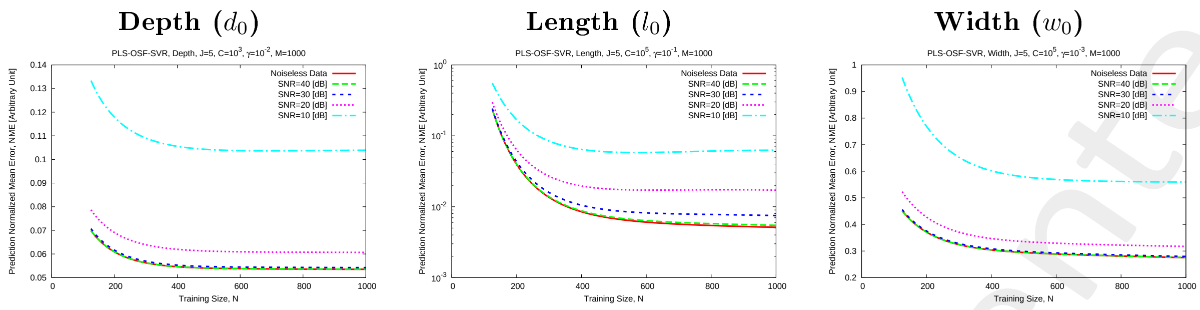

(a) (b) (c)

Figure 5: **PLS-OSF-SVR** - Normalized Mean Error (NME) vs. training size (N)

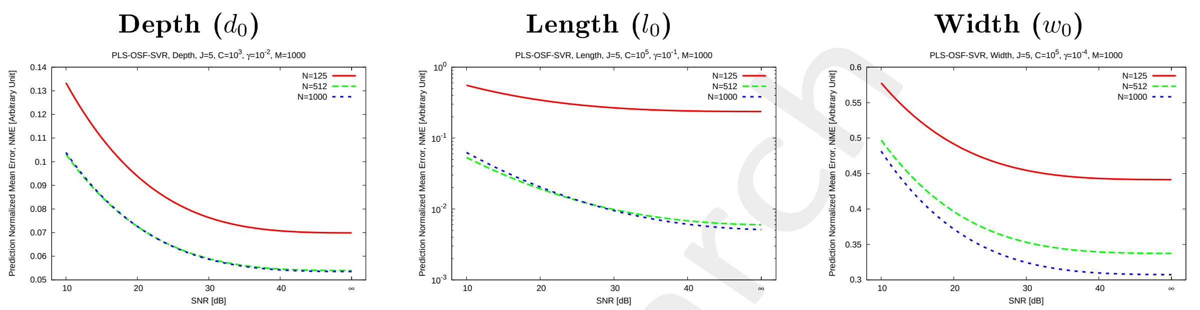

(a) (b) (c)

Figure 6: **PLS-OSF-SVR** - Normalized Mean Error (NME) vs. SNR on the test ECT measurements.

References

[1] M. Salucci, N. Anselmi, G. Oliveri, P. Calmon, R. Miorelli, C. Reboud, and A. Massa, "Real-time NDT-NDE through an innovative adaptive partial least squares SVR inversion approach," *IEEE Trans. Geosci. Remote Sens.*, vol. 54, no. 11, pp. 6818-6832, Nov. 2016.

[2] M. Salucci, G. Oliveri, F. Viani, R. Miorelli, C. Reboud, P. Calmon, and A. Massa, "A learning-by-examples approach for non-destructive localization and characterization of defects through eddy current testing measurements," in *2015 IEEE International Symposium on Antennas and Propagation*, Vancouver, 2015, pp. 900-901.

[3] M. Salucci, S. Ahmed and A. Massa, "An adaptive Learning-by-Examples strategy for efficient Eddy Current Testing of conductive structures," in *2016 European Conference on Antennas and Propagation*, Davos, 2016, pp. 1-4.

[4] P. Rocca, M. Benedetti, M. Donelli, D. Franceschini, and A. Massa, "Evolutionary optimization as applied to inverse problems," *Inverse Probl.*, vol. 25, pp. 1-41, Dec. 2009.

[5] A. Massa, P. Rocca, and G. Oliveri, "Compressive sensing in electromagnetics - A review," *IEEE Antennas Propag. Mag.*, pp. 224-238, vol. 57, no. 1, Feb. 2015.

[6] N. Anselmi, G. Oliveri, M. Salucci, and A. Massa, "Wavelet-based compressive imaging of sparse targets," *IEEE Trans. Antennas Propag.*, vol. 63, no. 11, pp. 4889-4900, Nov. 2015.

[7] M. Salucci, G. Oliveri, and A. Massa, "GPR prospecting through an inverse-scattering frequency-hopping multifocusing approach," *IEEE Trans. Geosci. Remote Sens.*, vol. 53, no. 12, pp. 6573-6592, Dec. 2015.

[8] T. Moriyama, G. Oliveri, M. Salucci, and T. Takenaka, "A multi-scaling forward-backward time-stepping method for microwave imaging," *IEICE Electron. Express*, vol. 11, no. 16, pp. 1-12, Aug. 2014.

[9] T. Moriyama, M. Salucci, M. Tanaka, and T. Takenaka, "Image reconstruction from total electric field data with no information on the incident field," *J. Electromagnet. Wave.*, vol. 30, no. 9, pp. 1162-1170, 2016.

[10] M. Salucci, L. Poli, and A. Massa, "Advanced multi-frequency GPR data processing for non-linear deterministic imaging," *Signal Processing - Special Issue on "Advanced Ground-Penetrating Radar Signal-Processing Techniques,"* vol. 132, pp. 306-318, Mar. 2017.